Supporting Information

Heterophase-Structured Bismuth Nanosheets for Solar Energy–Driven Electrocatalytic CO_2 Reduction to Formate†

Jian Zhang,[+] Chenchen Qin,[+] Daomeng Liu, Jiaxin He, Qingyi Li, Ziyi Feng, Zhiyuan Yang, Junzhong Wang,* Zhengkun Yang*

J. Zhang, C. Qin, D. Liu, J. He, Q. Li, Z. Feng, Z. Yang, Prof. J. Wang, Prof. Z. Yang
Institutes of Physical Science and Information Technology, Anhui Graphene Materials Research Center, Key Laboratory of Structure and Functional Regulation of Hybrid Materials of Ministry of Education, Anhui University, Hefei, 230601, China
E-mail: wangjz@ahu.edu.cn, yangzk@ustc.edu.cn

Computational details

All functional theory (DFT) method were performed using the Vienna *ab initio* simulation package (VASP) code with the projector augmented wave (PAW) method.[1, 2] The generalized gradient approximation (GGA) combined with Perdew-Burke-Ernzerhof (PBE) functional was employed to describe the exchange-correlation term.[3] The projector augmented wave (PAW) pseudo-potentials were used to describe ionic cores.[4] A vacuum space of 15 Å along the *z*-axis was added to avoid the interactions between periodic slabs. The cut-off energy for the plane-wave basis was set to 450 eV. The Van der Waals (vdW) interactions was described by using the empirical correction in Grimme's scheme (DFT-D3) in all calculations.[5] The convergence tolerances for energy and force were set to 10^{-5} eV and 0.05 eV/Å, respectively. The Gibbs free energy change (ΔG) for each elemental step was defined as

$\Delta G = \Delta E_{DFT} + \Delta E_{ZPE} - T\Delta S$

In this equation, ΔE_{DFT} is denotes the electronic energy change directly obtained from DFT calculations, ΔE_{ZPE} and ΔS are the zero-point energy correction and entropy change obtained from frequency calculations at 298.15 K.

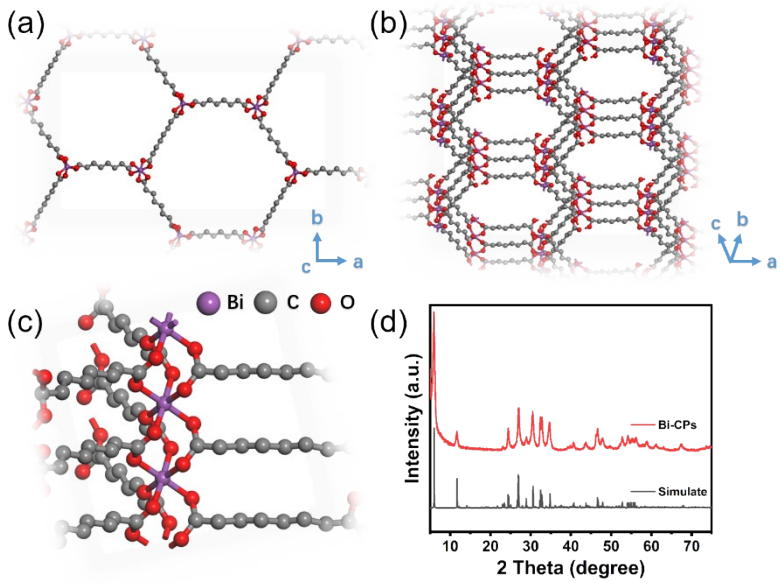

Fig. S1. (a, b) A model diagram of the possible structure of Bi-CPs from different perspectives. (c) Enlarged view of the coordination pattern between bismuth and ligand molecule. (d) XRD patterns of the simulated and as-prepared Bi-CPs.

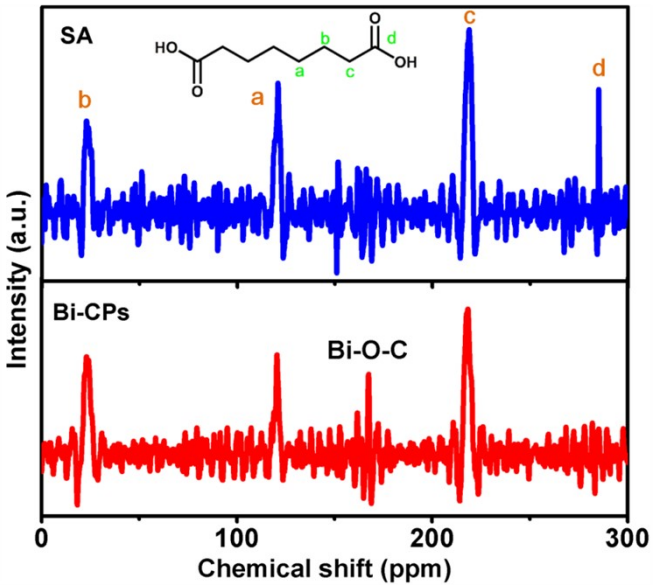

Fig. S2. ^{13}C NMR spectra of SA ligand and Bi-CPs powders.

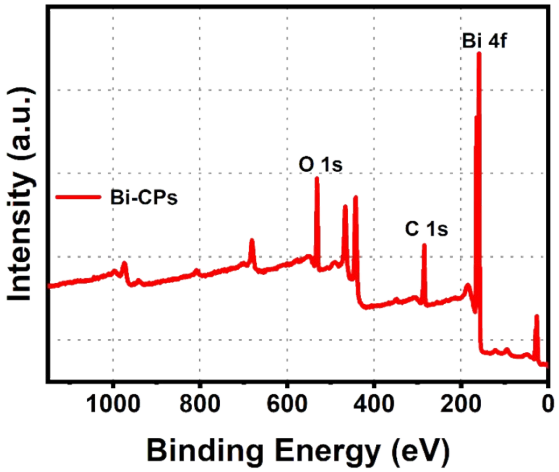

Fig. S3. The survey XPS spectrum of the as-synthesized Bi-CPs.

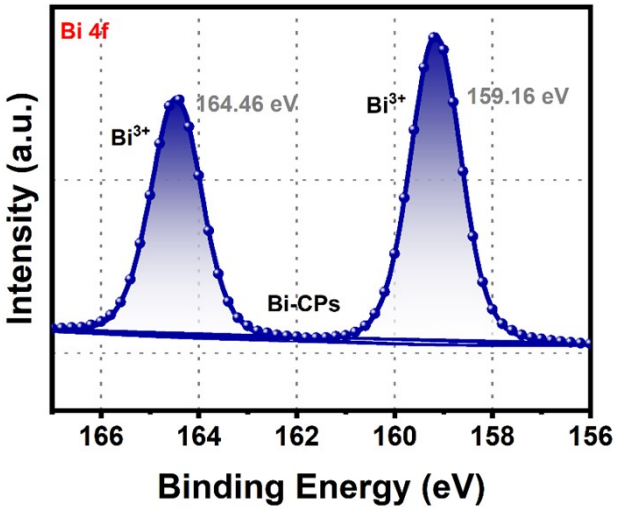

Fig. S4. The XPS of Bi 4f of the as-synthesized Bi-CPs.

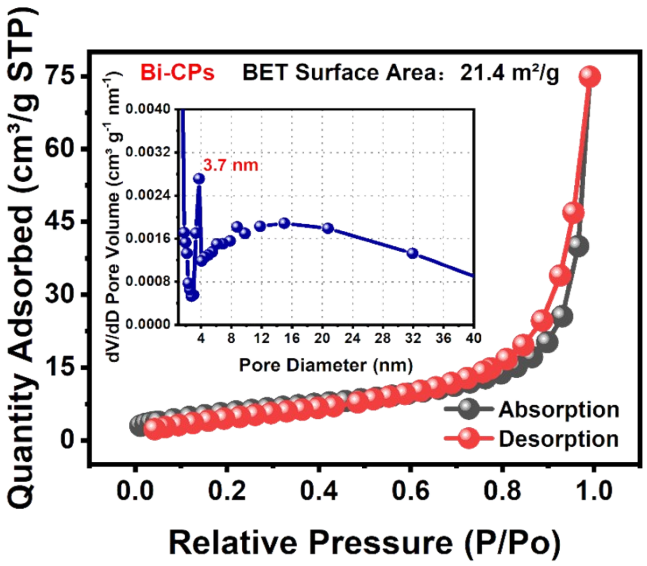

Fig. S5. N_2 adsorption-desorption isotherms (inset: pore size distribution) of the Bi-CPs.

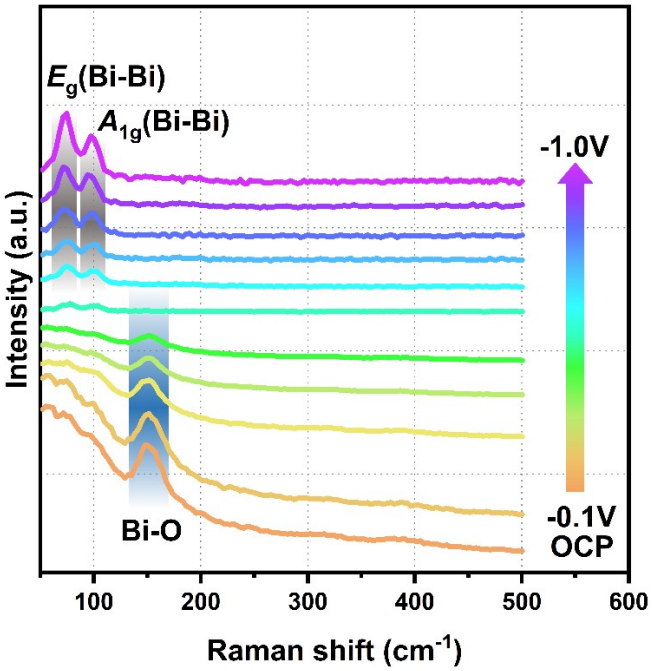

Fig. S6. In situ Raman spectroscopy recorded during the transformation from Bi-O to Bi under various applied potentials.

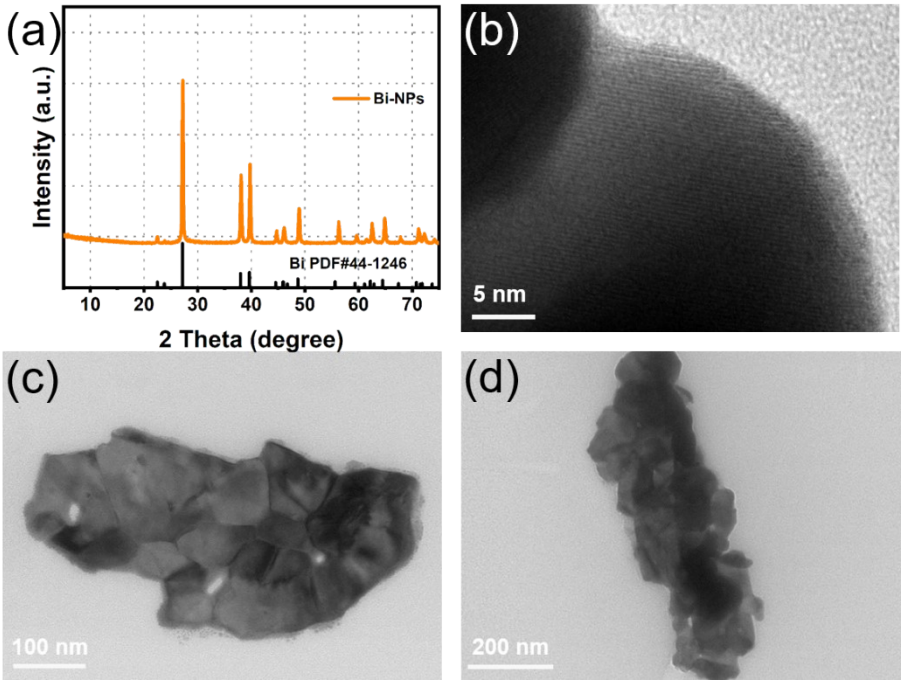

Fig. S7. The morphology and crystal structure of the as-synthesized Bi-NPs. (a) The XRD of Bi-NPs. (b) The HRTEM image of Bi-NPs. (c)(d) The TEM images of Bi-NPs.

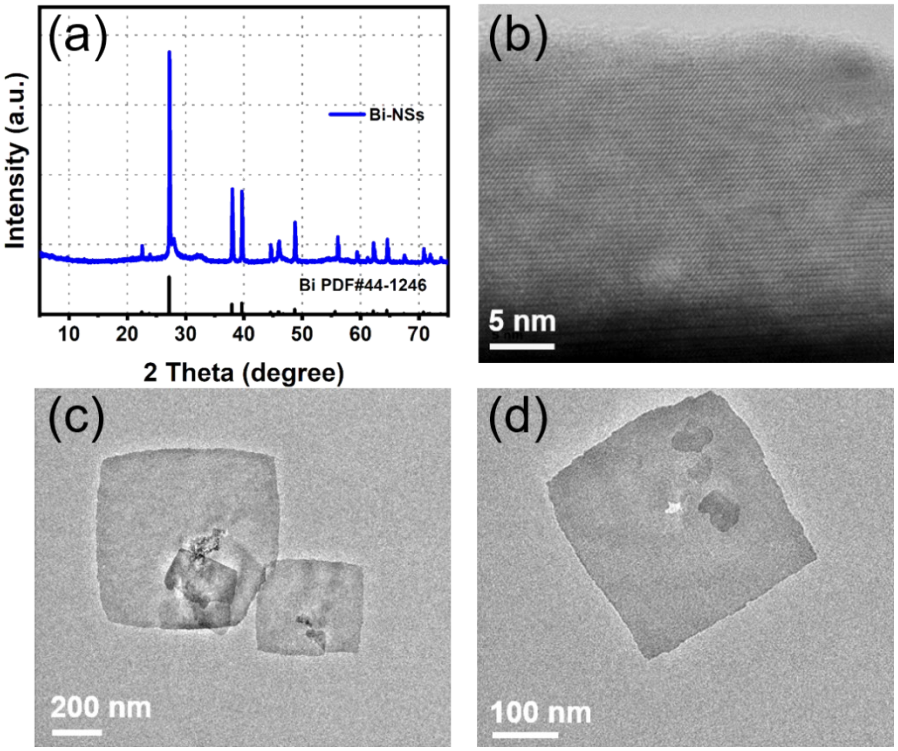

Fig. S8. The morphology and crystal structure of Bi-NSs. (a) The XRD of Bi-NSs. (b) The HRTEM image of Bi-NSs. (c)(d) The TEM images of Bi-NSs.

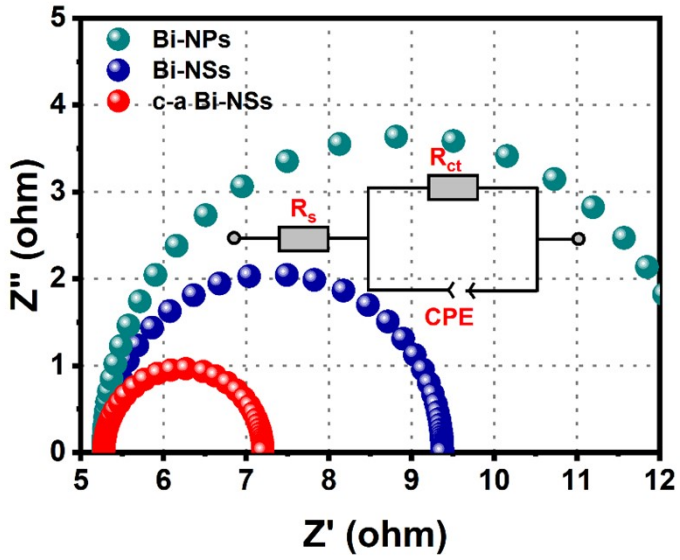

Fig. S9. Charge transfer resistance. EIS spectra of Bi-NPs, Bi-NSs and c-a Bi-NSs recorded at open circuit potential in the frequency range of 0.1 Hz−100kHz.

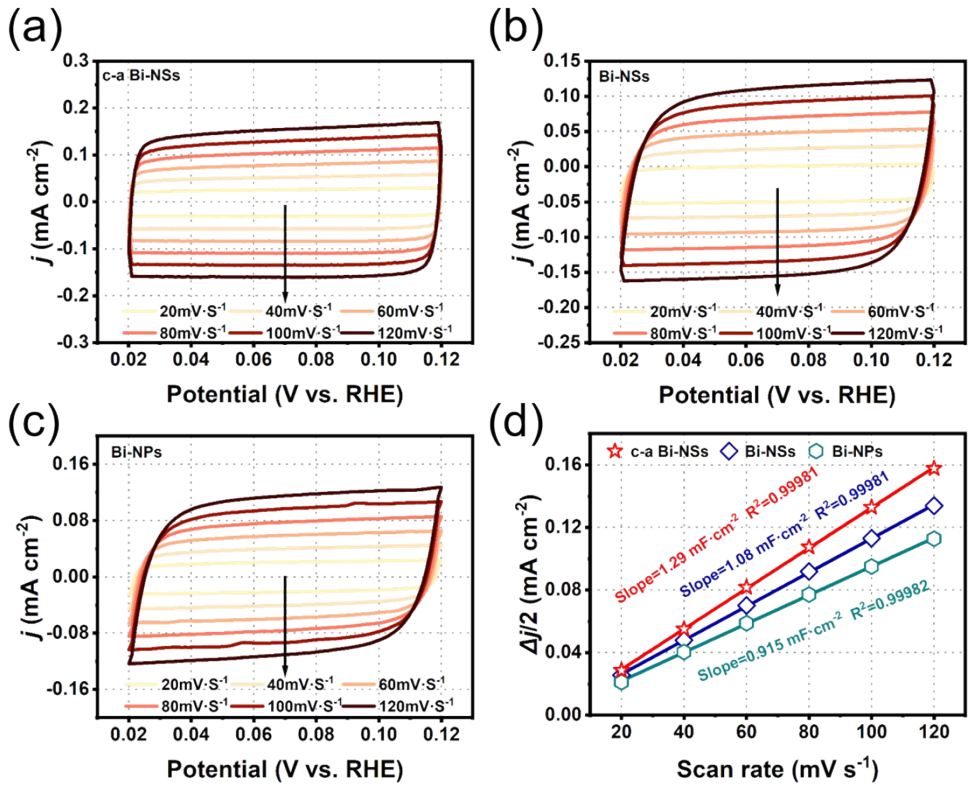

Fig. S10. CV curves of (a) c-a Bi-NSs, (b) Bi-NSs and (c) Bi NPs within the potential ranging from 0.02 to 0.04 V (vs. RHE) at various scan rates (20, 40, 60, 80, 100, 120 mV s^{-1}). (d) Plots of current density against scan rate.

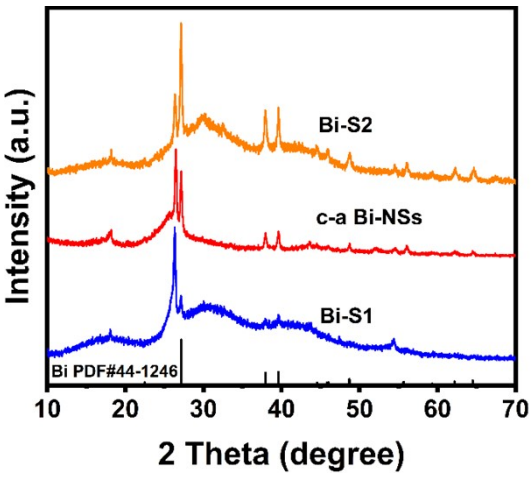

Fig. S11. XRD patterns of three types of Bi catalysts.

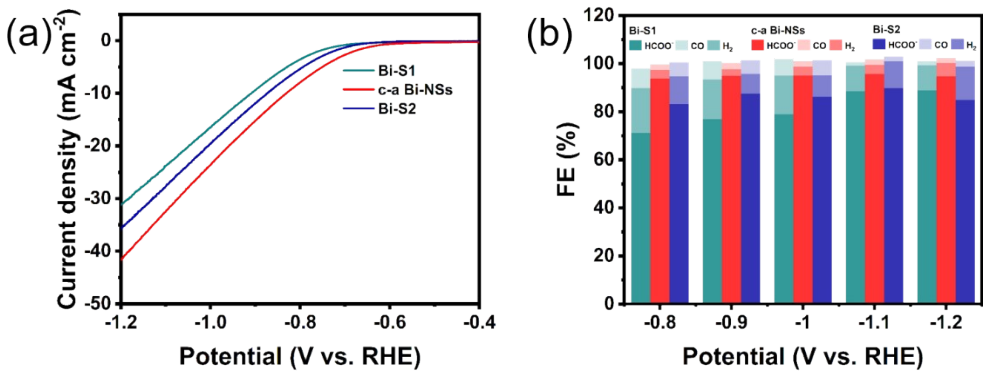

Fig. S12. (a) The LSV of different samples. (b) Faraday efficiency diagram of different samples.

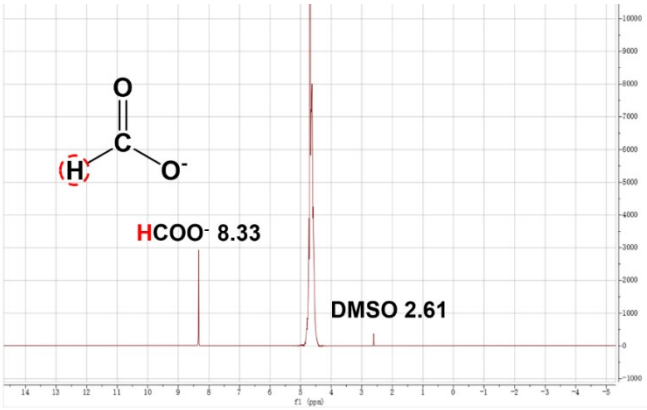

Fig. S13. The represent ^{1}H-NMR spectra of liquid product (DMSO as standard internal substance) obtained on the c-a Bi-NSs.

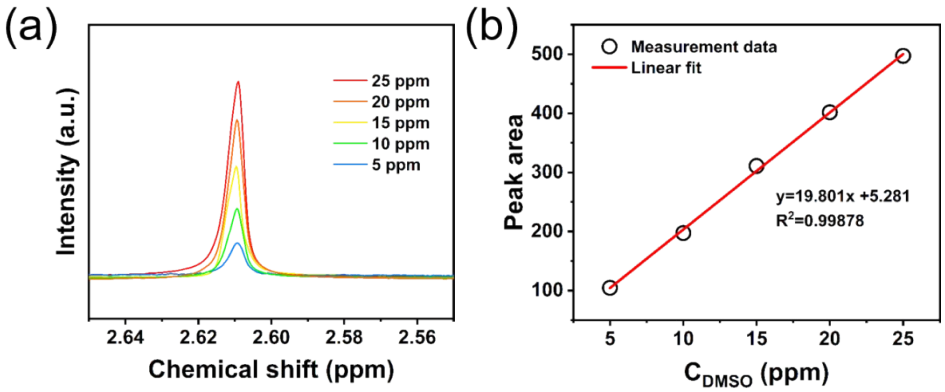

Fig. S14. (a) ^{1}H NMR spectra of DMSO at different concentrations. (b) The fitting curve of DMSO concentration with respect to peak-area.

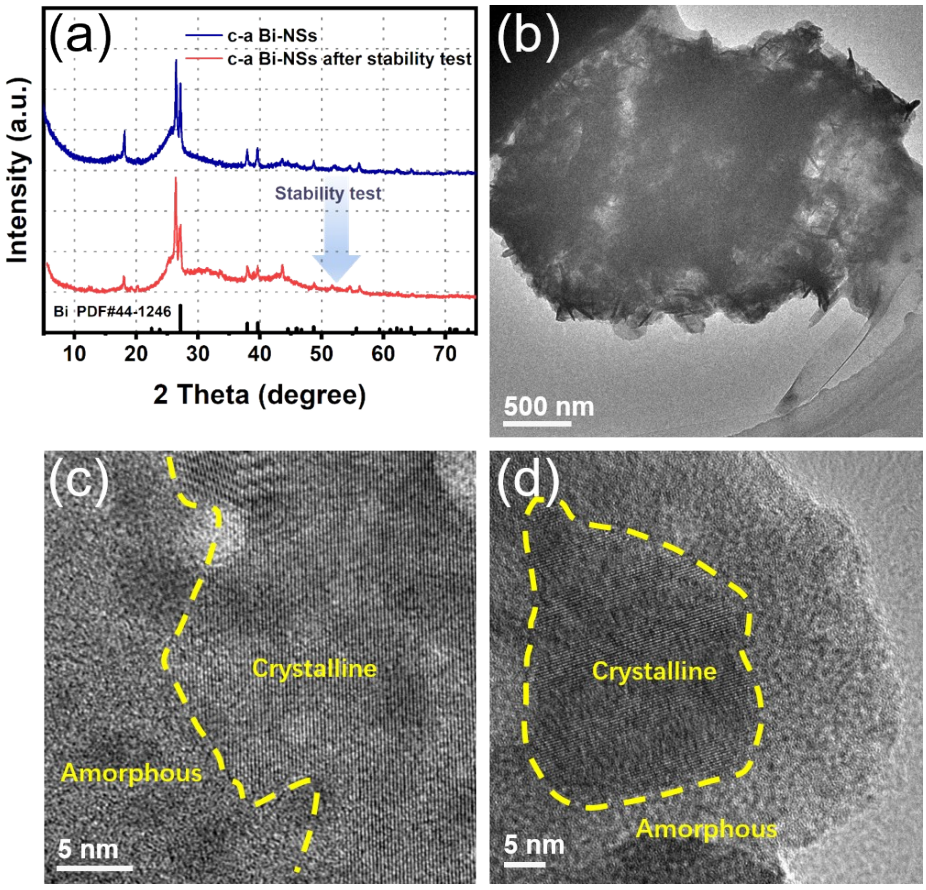

Fig. S15. (a) The XRD patterns of c-a Bi-NSs before and after stability test. (b) The TEM image of c-a Bi-NSs after stability test. (c)(d) The HRTEM images of c-a Bi-NSs after stability test.

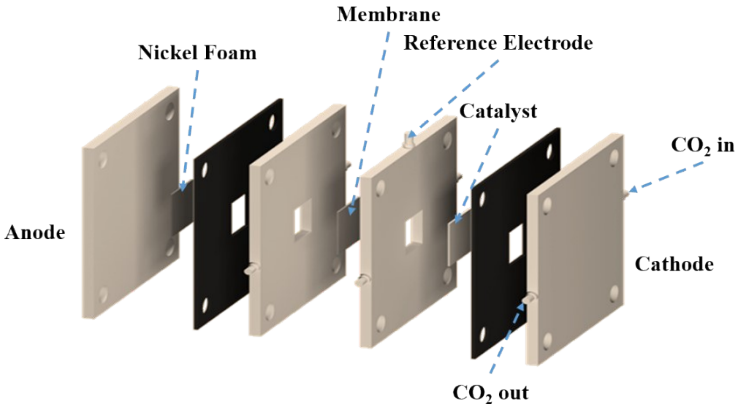

Fig. S16. The schematic diagram of flow cell.

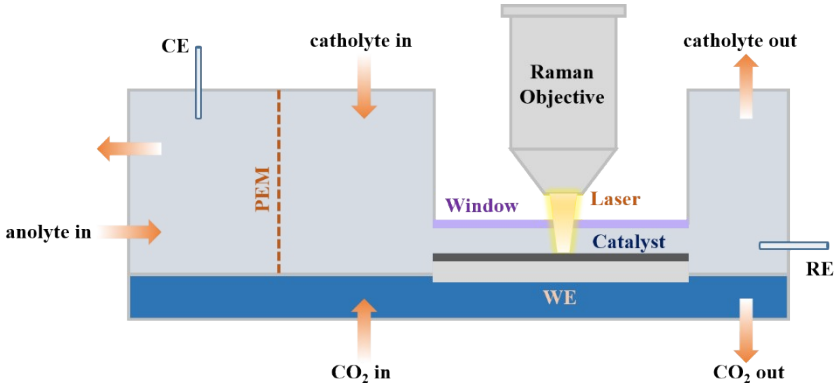

Fig. S17. Schematic illustration of in situ Raman characterization.

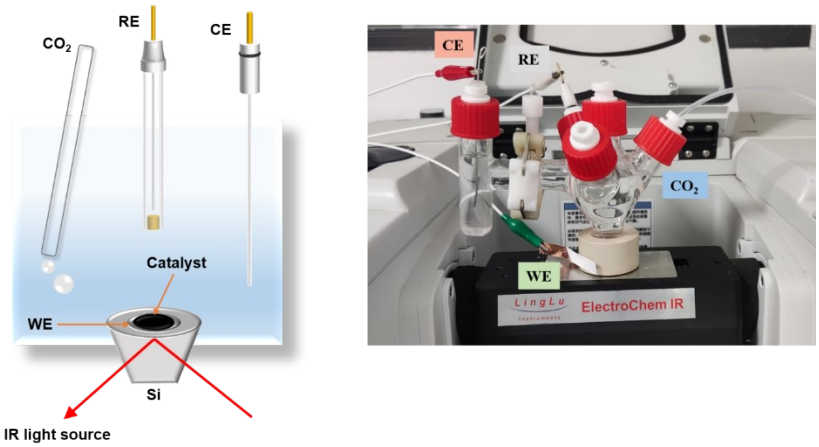

Fig. S18. (a) Schematic illustration of ATR-IR characterization and (b) Digital photograph showing the in-situ ATR-IR set-up.

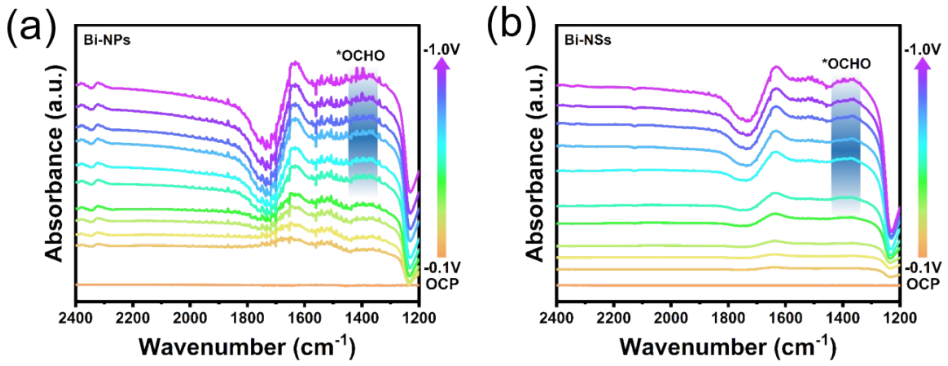

Fig. S19. In situ ATR-IR spectra on (a) Bi-NPs catalyst and (b) Bi-NSs catalyst.

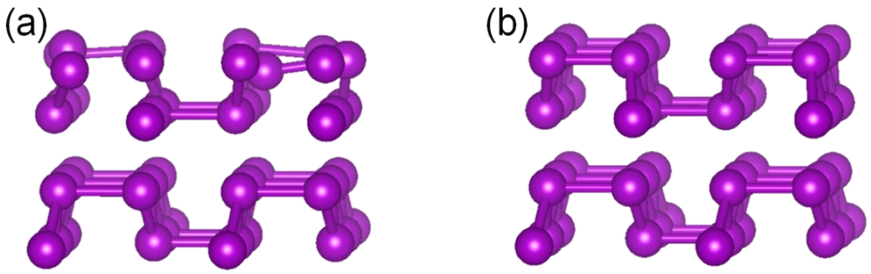

Fig. S20. The proposed theoretical models of (a) c-a Bi (110) and (b) crystalline Bi (110).

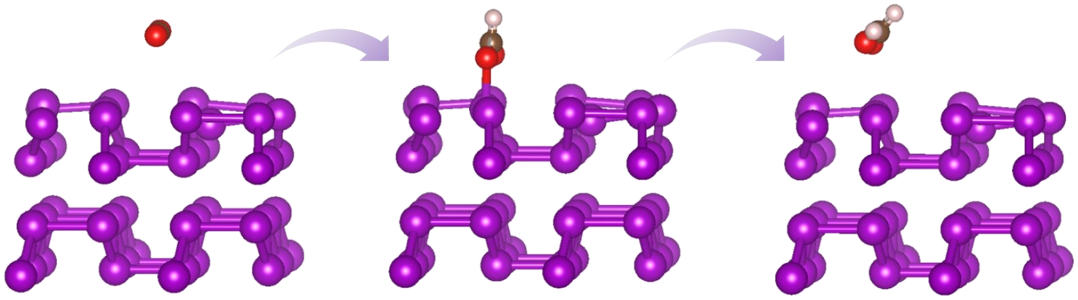

Fig. S21. The proposed electrochemical CO_2RR pathways over c-a Bi-NSs.

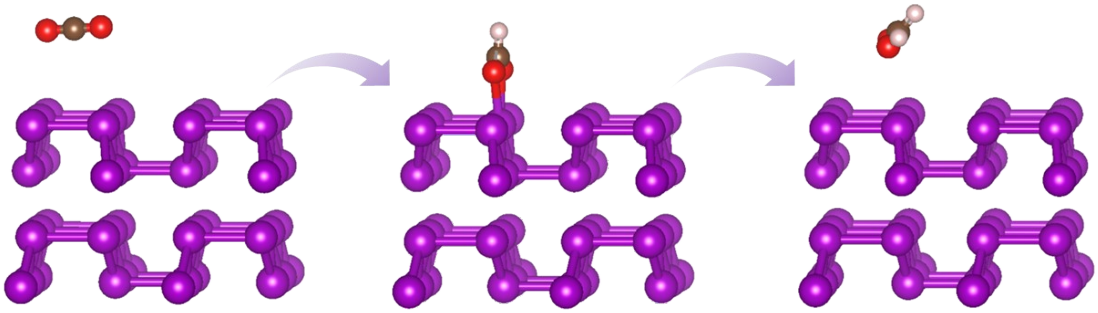

Fig. S22. The proposed electrochemical CO_2RR pathways over Bi-NSs.

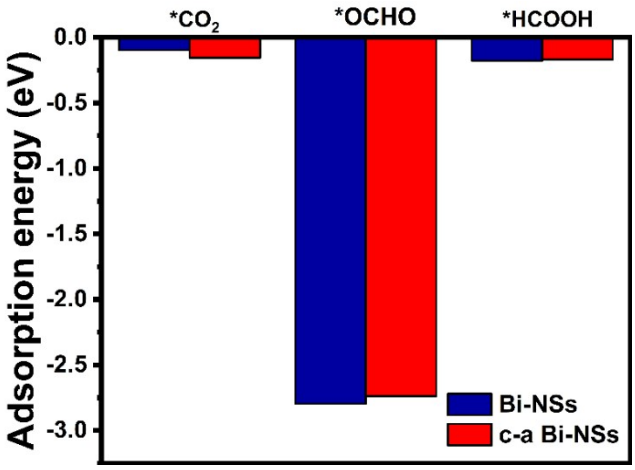

Fig. S23. The adsorption energy of key intermediates.

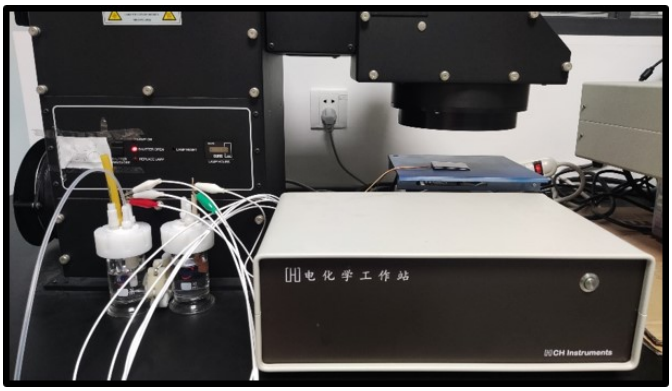

Fig. S24. Digital photo of the real photovoltaic-electrolysis system.

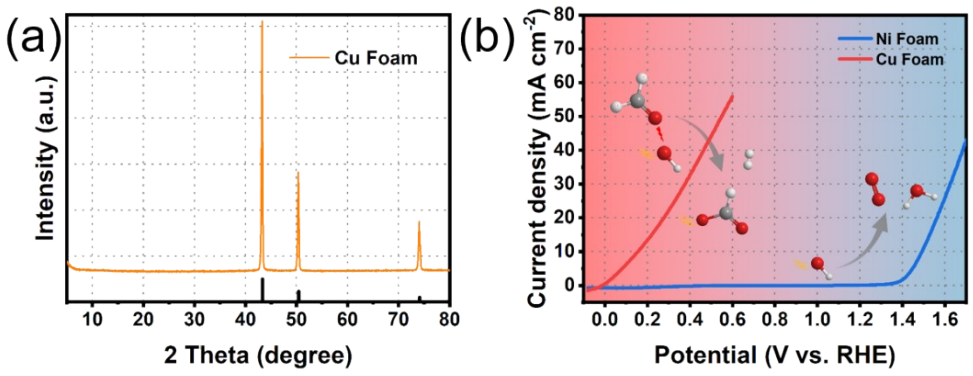

Fig. S25. (a) The XRD pattern of the Cu foam. (b) LSV curves of Cu foam (red) and Ni foam (blue) in 1 M KOH + 0.1 M HCHO.

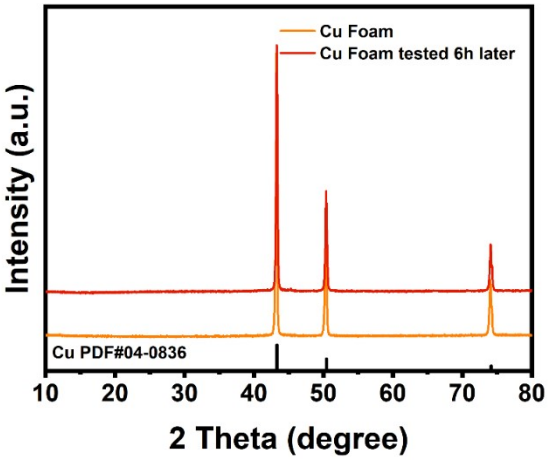

Fig. S26. The XRD pattern of Cu foam before and after 6h testing.

Table S1. Current density and FE over the reported materials for CO_2 reduction to $HCOO^-$ in H-type cell.

Catalyst	Electrolyte	Potential (V vs. RHE)	FE_{HCOO^-} (%)	J_{HCOO^-} (mA cm^{-2})	Potential range for FE_{HCOO^-} >90% (mV)	Reference
c-a Bi-NSs	**0.5 M $KHCO_3$**	**-1.10**	**95.6**	**33.4**	**600**	**This Work**
Cu-Bi	0.5 M $KHCO_3$	-1.00	92.5	49.5	~200	[6]
S-Bi-NSs	0.5 M $KHCO_3$	–0.88	95.3	19.4	400	[7]
Pits-Bi	0.1 M $KHCO_3$	-1.10	95.3	27.9	~200	[8]
SOR Bi@C NPs	0.5 M $KHCO_3$	-0.99	95.0	10.5	440	[9]
3.5nm Bi NS	0.1 M $KHCO_3$	-1.10	92.0	~10	~220	[10]
PD-Bi1	0.5 M $KHCO_3$	-0.90	91.4	~7	~200	[11]
Bi_2O_3@C-800	0.5 M $KHCO_3$	−0.90	92.0	7.5	~200	[12]
BMNS	0.5 M $KHCO_3$	-0.80	98.0	23	300	[13]
Bi(btb)	0.5 M $KHCO_3$	−0.97	95.0	~5.5	~200	[14]

Table S2. Current density and FE over the reported materials for CO_2 reduction to $HCOO^-$ in flow cell.

Catalysis	Electrolyte	Current density ($mA\ cm^{-2}$)	FE_{HCOO^-} (%)	Reference
c-a Bi-NSs	**1.0 M KOH**	**300**	**90.11**	**This Work**
BOC with V_O	1.0 M KOH	200	81	[15] *Nat. Commun.* **2023**, *14*, 751
Bi_2O_3/BiO_2	0.5 M $KHCO_3$	114	98.12	[16] *Nano Lett.* **2022**, *22*, 1656-1664
Sn-N-C	0.5 M $KHCO_3$	200	50-60	[17] *J. CO_2 Util.* **2021**, *50*, 101583.
Bi-NSs	1.0 M KOH	405	89	[18] *Adv. Energy Mater.* **2020**, *10*, 2001709
Bi_2O_3@C-800	1.0 M KOH	224	93	[12] *Angew. Chem. Int. Ed.* **2020**, *59*, 10807-10813
Bi-NBs	1.0 M KOH	200	95	[19] *Adv. Funct. Mater.* **2022**, *32*, 2201125
$Bi_{0.1}Sn$	1.0 M KOH	200	97	[20] *Nat. Commun.* **2021**, *12*, 5223.
SnO_2 NPs	1.0 M KOH	147	46	[21] *J. Mater. Chem. A* **2018**, *6*, 10313-10319
BiNN-CFs	1.0 M KOH	200	95.7	[22] *Adv. Energy Mater.* **2022**, *12*, 2103960
Bi-ene-NW	1.0 M KOH	200	95	[23] *Energy Environ. Sci.*, **2021**, *14*, 4998–5008
Bi_2O_3@C/HB	1.0 M KOH	250	93	[24] *ACS Nano*, **2021**, *15*, 17757−17768
CDB	1.0 M KOH	200	92	[25] *Adv. Energy Mater.* **2022**, 2202818
Ti-Bi-NSs	1.0 M KOH	130	93	[26] *Small*, **2023**, *19*, 2302253
basal-oriented Bi NSs	0.5 M $KHCO_3$	90	94	[27] *Appl. Catal. B: Environ.* **2021**, *299*, 120693

References

1. G. Kresse, J. Furthmüller, *Phys. Rev. B,* 1996, **54**, 11169-11186.
2. G. Kresse and D. Joubert, *Phys. Rev. B*, 1999, **59**, 1758-1775.
3. J. P. Perdew, K. Burke and M. Ernzerhof, *Phys. Rev. Lett.*, 1996, **77**, 3865-3868.
4. S. Grimme, J. Antony, S. Ehrlich and H. Krieg, *J. Chem. Phys.*, 2010, **132**, 154104.
5. J. Zhang, H. Zhang, H. Ye and Y. Zheng, *J. Chem. Phys.*, 2016, **145**, 094104.
6. Z. Li, B. Sun, D. Xiao, Z. Wang, Y. Liu, Z. Zheng, P. Wang, Y. Dai, H. Cheng and B. Huang, *Angew. Chem. Int. Ed.*, 2023, **62**, e202217569.
7. C.-J. Peng, G. Zeng, D.-D. Ma, C. Cao, S. Zhou, X.-T. Wu and Q.-L. Zhu, *ACS Appl. Mater. Interfaces*, 2021, **13**, 20589-20597.
8. Y. Yuan, Q. Wang, Y. Qiao, X. Chen, Z. Yang, W. Lai, T. Chen, G. Zhang, H. Duan, M. Liu and H. Huang, *Adv. Energy Mater.*, 2022, **12**, 2200970.
9. S. Liu, Y. Fan, Y. Wang, S. Jin, M. Hou, W. Zeng, K. Li, T. Jiang, L. Qin, Z. Yan, Z. Tao, X. Zheng, C. Shen, Z. Liu, T. Ahmad, K. Zhang and W. Chen, *Nano Lett.*, 2022, **22**, 9107-9114.
10. D. Yao, C. Tang, A. Vasileff, X. Zhi, Y. Jiao and S.-Z. Qiao, *Angew. Chem. Int. Ed.*, 2021, **60**, 18178-18184.
11. Y. Wang, Y. Li, J. Liu, C. Dong, C. Xiao, L. Cheng, H. Jiang, H. Jiang and C. Li, *Angew. Chem. Int. Ed.*, 2021, **60**, 7681-7685.
12. P. Deng, F. Yang, Z. Wang, S. Chen, Y. Zhou, S. Zaman and B. Y. Xia, *Angew. Chem. Int. Ed.*, 2020, **59**, 10807-10813.
13. N. Li, P. Yan, Y. Tang, J. Wang, X.-Y. Yu and H. B. Wu, *Appl. Catal. B: Environ.*, 2021, **297**, 120481.
14. P. Lamagni, M. Miola, J. Catalano, M. S. Hvid, M. A. H. Mamakhel, M. Christensen, M. R. Madsen, H. S. Jeppesen, X.-M. Hu, K. Daasbjerg, T. Skrydstrup and N. Lock, *Adv. Funct. Mater.*, 2020, **30**, 1910408.
15. X. Chen, J. Chen, H. Chen, Q. Zhang, J. Li, J. Cui, Y. Sun, D. Wang, J. Ye and L. Liu, *Nat. Commun.*, 2023, **14**, 751.
16. X. Feng, H. Zou, R. Zheng, W. Wei, R. Wang, W. Zou, G. Lim, J. Hong, L. Duan and H. Chen, *Nano Lett.*, 2022, **22**, 1656-1664.
17. M. Duarte, N. Daems, J. Hereijgers, D. Arenas-Esteban, S. Bals and T. Breugelmans, *J. CO_2 Util.*, 2021, **50**, 101583.
18. J. Yang, X. Wang, Y. Qu, X. Wang, H. Huo, Q. Fan, J. Wang, L.-M. Yang and Y. Wu, *Adv. Energy Mater.*, 2020, **10**, 2001709.
19. G. Zeng, Y. He, D.-D. Ma, S. Luo, S. Zhou, C. Cao, X. Li, X.-T. Wu, H.-G. Liao and Q.-L. Zhu, *Adv. Funct. Mater.*, 2022, **32**, 2201125.
20. L. Li, A. Ozden, S. Guo, F. P. García de Arquer, C. Wang, M. Zhang, J. Zhang, H. Jiang, W. Wang, H. Dong, D. Sinton, E. H. Sargent and M. Zhong, *Nat. Commun.*, 2021, **12**, 5223.
21. C. Liang, B. Kim, S. Yang, L. Yang, C. Francisco Woellner, Z. Li, R. Vajtai, W. Yang, J. Wu, P. J. A. Kenis and Pulickel M. Ajayan, *J. Mater. Chem. A*, 2018, **6**, 10313-10319.
22. B. Wulan, L. Zhao, D. Tan, X. Cao, J. Ma and J. Zhang, *Adv. Energy Mater.*, 2022, **12**, 2103960.
23. M. Zhang, W. Wei, S. Zhou, D.-D. Ma, A. Cao, X.-T. Wu and Q.-L. Zhu, *Energy Environ. Sci.*, 2021, **14**, 4998-5008.
24. S.-Q. Liu, E. Shahini, M.-R. Gao, L. Gong, P.-F. Sui, T. Tang, H. Zeng and J.-L. Luo, *ACS Nano*, 2021, **15**, 17757-17768.
25. H. Shen, Y. Zhao, L. Zhang, Y. He, S. Yang, T. Wang, Y. Cao, Y. Guo, Q. Zhang and H. Zhang, *Adv. Energy Mater.*, 2023, **13**, 2202818.
26. A. Xu, X. Chen, D. Wei, B. Chu, M. Yu, X. Yin and J. Xu, *Small*, 2023, **19**, 2302253.
27. W. Dan, K. Chang, Y. Zhang, Y. Wang, Q. Liu, Z. Wang, D. Ding, Y. Cui, C. Pan, Y. Lou, Y. Zhu and Y. Zhang,

Appl. Catal. B: Environ., 2021, **299**, 120693.